Seed-Mediated Electrodeposition of Silver Nanowires (NWs) and Nanorods (NRs)

Nidhi Shaha*, Tien-Lu Huanga, Harikrishnan N. Nambiarb, Francis P. Zamborinib

^aDepartment of Chemistry, Indiana University Southeast, New Albany, Indiana 47150, United States

^bDepartment of Chemistry, University of Louisville, Louisville, Kentucky 40292, United States *E-mail: snidhi@iu.edu

ABSTRACT

Here we compare the amount and morphology of silver (Ag) nanostructures electrodeposited at varied potential and time in the presence of cetyltrimethylammonium bromide (CTAB) onto glass/indium tin oxide (glass/ITO) electrodes functionalized with mercaptopropyltrimethoxysilane (MPTMS) and coated or not coated with 4 nm average diameter Au nanoparticle (Au NP) seeds. There is a significantly larger amount of Ag deposited on the seeded electrode surface compared to the non-seeded electrode at potentials of -150 mV to -300 mV (vs. Ag/AgCl) since the Au NP seeds act as catalysts for Ag deposition. At more negative overpotentials of -400 to -500 mV, the amount of Ag deposited on both electrodes is similar because the deposition kinetics are fast enough on glass/ITO that the Au seed catalyst does not make as big of a difference. Ag nanorods (NRs) and nanowires (NWs) form on the seeded surfaces, especially at more positive potentials, where deposition primarily occurs on the Au seed catalysts. Deposition of Ag onto the Au seeds appears as a separate peak in the

voltammetry. This procedure mimics the seed-mediated growth of Ag NRs observed in solution in the presence of CTAB using ascorbic acid as a reducing agent. The yield, length, and aspect ratio of the Ag NRs/NWs depends on the deposition time and potential with the average length ranging from 300 nm to 3 µm for times of 30 to 120 min and potentials of -150 mV to -200 mV. The electrochemical seed-mediated growth of Ag NRs/NWs across electrode gaps could find use for resistive and surface-enhanced Raman-based sensing and molecular electronics applications.

INTRODUCTION

It is well known that the optical, magnetic, electrochemical, catalytic, and electronic properties of metal nanoparticles (NPs) depend on their size, shape, and composition. Onedimensional (1D) nanostructures are one particular shape that has received a great deal of attention over the years. In particular, 1D nanorods (NRs) and nanowires (NWs) play an important role in fabricating nanoscale electronic, ², ³ optoelectronic, ⁴ sensing, ^{5,6} and plasmonic devices.^{7,8} These types of 1D nanostructures can be synthesized by electrochemical, templateassisted, and seed-mediated methods. The wet chemical and seed-mediated method developed by the groups of Murphy and El-Sayed has emerged as the most versatile. 9, 10 Murphy and coworkers developed a solution method for synthesizing 1D metal (NRs) and NWs in solution using the seed-mediated growth method, where surfactants directed the 1D growth. 10-13 Alternatively, 1D nanostructures can be fabricated or synthesized directly on surfaces. Direct synthesis of 1D nanostructures can be achieved chemically or electrochemically from seed nanoparticles that are directly attached to surfaces or from surface templates. 14 Taub et al described the surfactant-directed synthesis of Au nanorods (NRs) directly on mica from surfacebound Au nanoparticle seeds. 15 Our group used a similar approach to synthesize surfaceattached Au NRs on functionalized Si/SiO_x surfaces, where we manipulated the NRs, followed

the growth by atomic force microscopy (AFM), formed patterns of Au NR surfaces, and fabricated highly-aligned Au NRs on surfaces. ¹⁶⁻¹⁹ More recently, Neretina and co-workers reported the synthesis of high yield arrays of Au nanoplates by chemical seed-mediated growth directly on surfaces, demonstrating the synthesis of other shapes as well. ²⁰

Our group also synthesized Au NRs directly on surfaces by seed-mediated growth using electrochemical potential (electrodeposition) in place of a chemical reducing agent.²¹ The surfactant cetyltrimethylammonium bromide (CTAB) directed the NR shape as Au NP seeds grow by electrodeposition at the electrode surface. Others have synthesized NRs and NWs electrochemically in hard templates, including porous membranes,²² the step-edges of graphite,⁵ or at the edges of thin nickel films patterned by lithography, which is termed lithographically patterned nanowire electrodeposition (LPNE).²³ There are various examples of electrochemical seed-mediated growth of other nanostructures.²⁴ For example, Raj and John showed the growth of Au NRs on electrode surfaces using electrochemical seed-mediated approach on electrochemically formed Au seeds.²⁵ Nambiar and Zamborini showed that the kinetics for Au electrodeposition from HAuCl₄ is faster on Au seed nanoparticles (NPs) compared to glass/ITO and that the rate of electrodeposition increased with decreasing Au NP size. 26 Song and coworkers electrodeposited Cu onto Ag nanocube seeds and followed the process by real-time single-particle imaging.²⁷ More recently, Ringe and co-workers electrodeposited Cu onto Au nanocube seeds, forming multilobed structures with tracking by dark-field scattering.²⁸ Seedmediated electrodeposition is clearly a relevant method for metal nanostructure engineering.

Here we describe the synthesis of Ag NRs/NWs on indium tin oxide-coated glass (glass/ITO) electrodes coated with Au seed NPs by the seed-mediated electrodeposition of Ag from Ag⁺ in the presence of CTAB. We used a similar approach as the seed-mediated electrodeposition

approach used by Abdelmoti and Zamborini to synthesize Au NRs/NWs directly on electrode surfaces.²¹ This work is important for two main reasons. First, our method allows the direct synthesis and assembly of Ag NRs/NWs directly on electrode surfaces, which could be useful for electrocatalysis, electrochemical sensing, electrooptical, SERS, and nanoelectronic studies. Second, extending our method of synthesizing 1D nanostructures directly on surfaces to Ag and other metals or alloys could open the door for their use in many different applications.

EXPERIMENTAL SECTION

Chemicals. Cetyltrimethylammonium bromide (CTAB, \geq 97.0%), silver nitrate (AgNO₃, \geq 99%), trisodium citrate (\geq 99.0%), 4-aminothiophenol (4-ATP, 97%), phenol (99%), 1,8-octanedithiol (\geq 97%), sodium borohydride (NaBH₄, 98.0%), mercaptopropyltrimethoxysilane (MPTMS, \geq 97.0%), isopropyl alcohol (99.8%) and acetone (99.9+%) were purchased from Sigma-Aldrich. Ethanol (100%) was purchased from Decon Laboratories, Inc. Sodium phosphate dibasic (98%) was purchased from EMD chemicals and sodium phosphate tribasic (98%) was purchased from Allied Chemicals. H₂SO₄ was purchased from VWR. Water purified to a resistivity of 18 MΩ-cm with a Barnstead NANOpure ultrapurification system was used for all aqueous solutions. HAuCl₄-3H₂O was synthesized from 99.99% metallic Au in our laboratory.

Synthesis of Au seed nanoparticles (NPs). A solution of 2.5×10^{-4} M citric acid trisodium salt and 2.5×10^{-4} M HAuCl₄ was prepared by combining 2.5 mL of 0.01 M citric acid trisodium salt, 2.5 mL of 0.01 M HAuCl₄, and 95 mL of purified water with a resistivity of 18 M Ω -cm, which gave a yellow solution. Then, 3.0 mL of 0.1 M ice-cold NaBH₄ was added to the solution, turning the color from yellow to reddish brown, indicating the formation of Au seed NPs. The solution was allowed to stir for 2 h prior to use. This seed solution contained 4 nm average-

diameter citrate-capped Au NPs based on Transmission Electron Microscopy (TEM) imaging. ^{13,}
²⁹ The UV-vis spectrum shows a localized surface plasmon resonance (LSPR) peak at 509 nm,
which is consistent with 4 nm diameter citrate-stabilized Au NPs as shown in the Supporting
Information Figure S1.

Electrode Modification. Single-sided 7 mm x 50 mm x 0.9 mm indium tin oxide (ITO) – coated glass (glass/ITO) electrodes with an 8-12 Ω resistance (Delta Technologies, Loveland, CO) were cleaned by sonication for 10 min each in water purified to a resistivity of 18 MΩ-cm, acetone, and isopropyl alcohol sequentially. The cleaned glass/ITO electrode was functionalized by immersion for 20 min in a solution containing 10 mL of isopropyl alcohol, 1 to 2 drops of water, and 100 μL of mercaptopropyltrimethoxysilane (MPTMS) that was heated to 50-60 9 C. This led to a surface terminated with thiol groups. The glass/ITO/MPTMS was then rinsed and sonicated for 10 min in isopropyl alcohol and dried under N₂ before being immersed in a solution of 4 nm diameter Au NPs for 20 min, which led to the attachment of the Au NPs to the glass/ITO/MPTMS surface through strong Au-thiolate covalent interaction. The resulting glass/ITO/MPTMS/Au NP (4 nm) electrode was rinsed with purified water with a resistivity of 18 MΩ-cm and dried under N₂ before electrochemical studies. These electrodes were used for experiments involving the electrochemical seed-mediated growth of Ag nanorods (NRs) and nanowires (NWs).

Cyclic Voltammetry. CVs of glass/ITO/MPTMS and glass/ITO/MPTMS/Au NP seed were obtained in pH 10.6 phosphate-buffered 0.1 M CTAB plus 2.5 x 10⁻⁴ M AgNO₃ solution using a CH Instruments electrochemical workstation (Austin, TX) with an Ag/AgCl (3 M KCl) reference electrode and Pt wire counter electrode at a scan rate of 100 mV/s.

Ag Electrodeposition. The glass/ITO/MPTMS and glass/ITO/MPTMS/Au NP seed (4 nm) electrodes were used as two working electrodes along with an Ag/AgCl reference electrode and a Pt wire counter electrode in an electrochemical cell with a deposition solution containing pH 10.6 phosphate-buffered 2.5 x 10⁻⁴ M AgNO₃ plus 0.1 M CTAB electrolyte. Our procedure is similar to the previous method developed in our group for synthesizing Au NRs electrochemically onto glass/ITO electrode surfaces.²¹ Ag deposition was performed in cyclic voltammetry mode as follows. First, both the non-seeded and seeded electrodes were attached to the working electrode lead and held out of the solution while the reference and counter electrodes were placed into the deposition solution. The cyclic voltammogram showed no current response to varying potential with high cell resistance at the point where only the reference and counter electrode were placed in the solution. Next, with the two working electrodes still out of the solution, the potential was scanned from 200 mV to a final potential x, where x was varied from -100 mV to -500 mV. Once potential x was reached, it was held constant (paused) and the two working electrodes were lowered into the solution under potential control for an amount of time ranging from 30 to 120 min. After the desired time, both working electrodes were removed from the solution while the potential was still held constant at x, rinsed thoroughly with purified water and finally dried under N₂ prior to ASV and SEM characterization.

SEM Characterization. Scanning Electron Microscopy (SEM) images were obtained using a Carl Zeiss SMT AGSUPRA 35VP field emission scanning electron microscope operating at an accelerating voltage of 8.00 kV. SEM images directly provided information about the shape, size, and structure of the Ag NRs/NWs synthesized. Nanorod and nanowire lengths and widths were determined from top-down images. Some samples were treated by a "taping method" in order to remove spherical shaped Ag nanostructures from the electrode.^{30, 31} In this case, Scotch

tape adhesive was pressed firmly onto the glass/ITO/MPTMS/Au seed electrode after Ag deposition at -185 mV for 30 min, rinsing, and drying. The tape was then slowly removed at an ~90 degree angle from the electrode plane and imaged by SEM.

Anodic Stripping Voltammetry. The amount of Ag deposited onto the glass/ITO electrodes was analyzed by linear sweep anodic stripping voltammetry (ASV). The potential was scanned from 0.0 mV to 0.8 mV in 0.1 M H₂SO₄ solution with an Ag/AgCl (3 M KCl) reference electrode and Pt wire counter electrode at a scan rate of 100 mV/s. The amount of Ag on the sample was determined by integrating the charge under the stripping peak. We performed ASVs on samples after Ag deposition and plotted charge versus potential for each deposition time. The plot excludes a few trials for both non-seeded and seeded samples if one of the two electrodes had obvious issues, such as peaks not consistent with Ag oxidation, noise above the signal level caused by incorrect settings or poor connections between the leads and electrodes.

RESULTS AND DISCUSSION

Seed-mediated Electrodeposition. Seed-mediated Ag electrodeposition was performed on glass/ITO electrodes functionalized with mercaptopropyltrimethoxysilane (glass/ITO/MPTMS) coated with Au NP seeds. Electrodeposition took place in pH 10.6 phosphate buffer solution in the presence of 0.1 M CTAB plus 2.5 x 10⁻⁴ M AgNO₃, similar to our previous method for Au.²¹ Au NP seeds were synthesized by reduction of HAuCl₄ with borohydride in the presence of citrate.¹⁸ The seed synthesis resulted in NPs that were 3 to 5 nm in diameter. The Au NPs act as nucleation sites on the glass/ITO/MPTMS electrode to catalyze the electrochemical growth of Ag nanostructures. Figure 1 shows CVs of glass/ITO, glass/ITO/MPTMS and glass/ITO/MPTMS/Au seed in 2.5 x 10⁻⁴ M AgNO₃ plus 0.1 M CTAB solution buffered at pH

10.6. The most important observation from this experiment is that Ag deposition on seeded glass/ITO/MPTMS/Au NPs starts 700 to 800 mV more positive compared to glass/ITO and 500 mV more positive from glass/ITO/MPTMS, when considering the small reduction peak at about -150 mV, and there is no cross-over in the CV on the reverse scan at ~-900 mV and -570 mV, respectively. This positive shift in potential is due to the presence of Au seeds which act as nucleation sites that strongly catalyze Ag deposition. Based on this shift, deposition potentials were chosen in this region, which is well before the deposition of Ag onto the glass/ITO/MPTMS, to ensure that Ag deposition only occurred by seed-mediated growth on the Au NP seeds. The CV for glass/ITO/MPTMS/Au seed has a clear peak at -185 mV corresponding to the Ag deposition on Au NP seeds. The glass/ITO electrode has a peak potential near -980 mV,

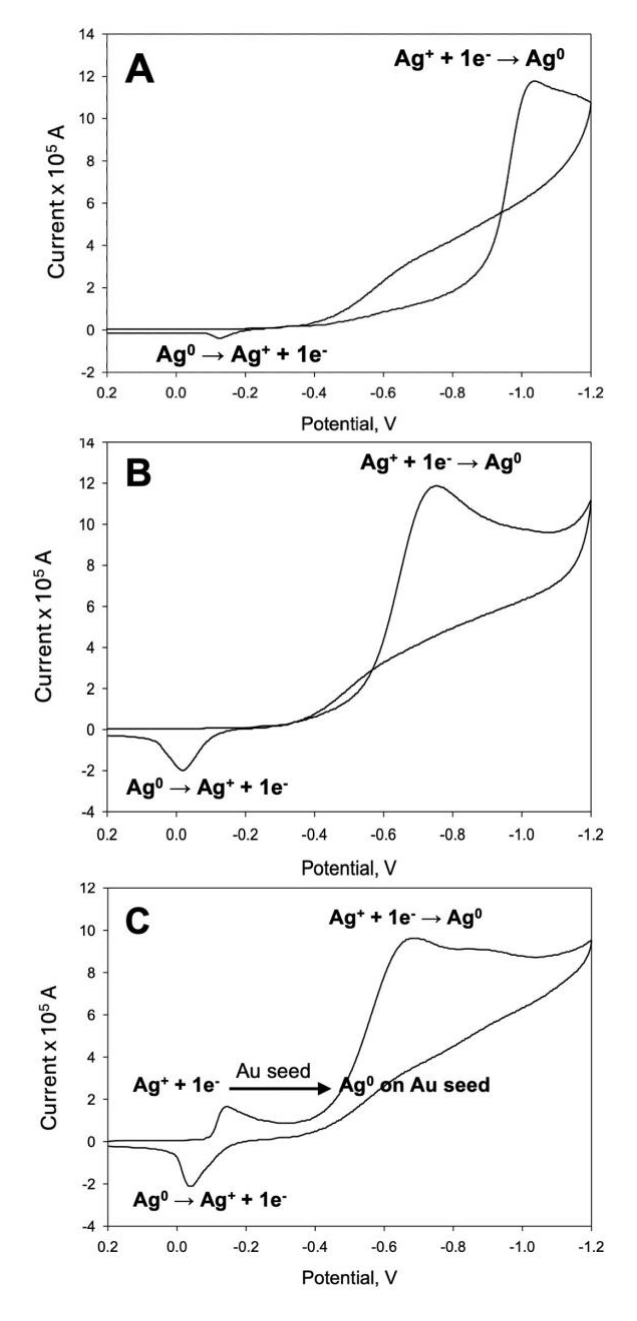


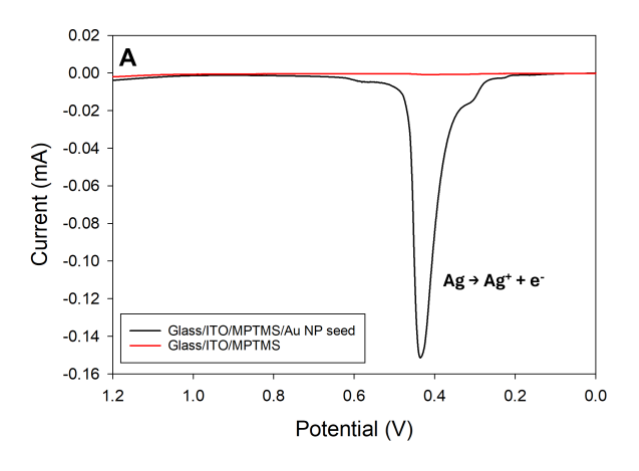
Figure 1. (A) CVs of glass/ITO, (B) glass/ITO/MPTMS and (C) glass/ITO/MPTMS/Au seed in pH 10.6 buffered 0.1 M CTAB plus 2.5 x 10⁻⁴ M AgNO₃ solution from 200 mV to -1200 mV.

which is almost -800 mV more negative. Also, on the reverse scan, the reduction current is

larger at more positive potentials than on the forward scan. This indicates a large overpotential

for initial Ag⁺ reduction to nucleate Ag and a smaller overpotential for Ag⁺ reduction for growth of the initial structures. The glass/ITO/MPTMS has a lower overpotential with peak potential at -750 mV, but similar higher reduction current and cross-over in the CV on the reverse scan. It is not clear why MPTMS shifts the deposition potential positive, but this is very interesting.

Anodic Stripping Voltammetry. We obtained ASV data for all the glass/ITO/MPTMS and glass/ITO/MPTMS/Au seed working electrodes after the Ag deposition procedure to determine the amount of Ag deposited on the surfaces as a function of electrode potential and time. Metallic Ag is stripped from the electrode using 0.1 M H₂SO₄ solution. Figure 2A shows the ASV of glass/ITO/MPTMS and glass/ITO/MPTMS/Au NP seeds after Ag electrodeposition for 30 min at -150 mV (see Figure S2 for other potentials). The glass/ITO/MPTMS



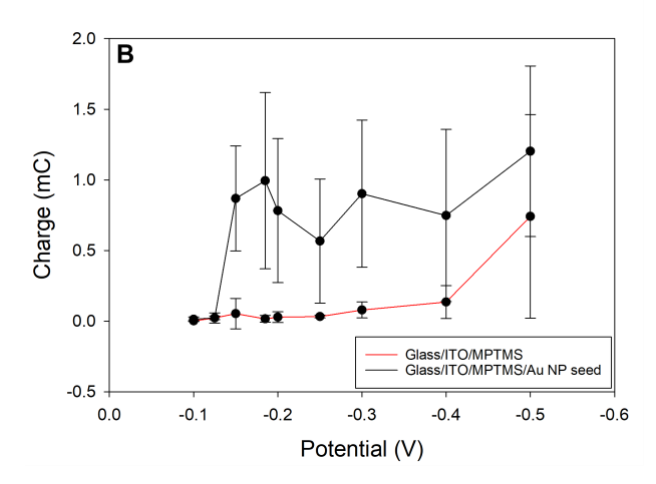


Figure 2. (A) ASV of glass/ITO/MPTMS (red) and glass/ITO/MPTMS/Au NP seeds (black) after deposition of Ag at E = -150 mV for 30 min. (B) Charge under the ASV peak(s) of glass/ITO/MPTMS (red) and glass/ITO/MPTMS/Au NP seed (black) electrodes held at different potentials for 30 min in pH 10.6 buffered 0.1 M CTAB plus 2.5 x 10⁻⁴ M AgNO₃ solution.

shows no peak while the glass/ITO/MPTMS/Au NP seed sample has a major peak at 430 mV. The peak is due to the oxidation of Ag by the following reaction.

$$Ag^0 \rightarrow Ag^+ + 1e^-$$
 (1)

Figure 2B shows the Ag stripping data (charge in Coulombs) of glass/ITO/MPTMS and glass/ITO/MPTMS/Au NP seed

obtained after Ag deposition for 30 min at potentials from -100 mV to -500 mV. Table S1 in the Supporting Information provides the average charge statistics for Ag stripping after Ag deposition at different potentials for a time of 30 minutes. For the seeded glass/ITO/MPTMS/Au NP electrodes (black line, open circles) the charge under the oxidation peak was much greater than that for the non-seeded

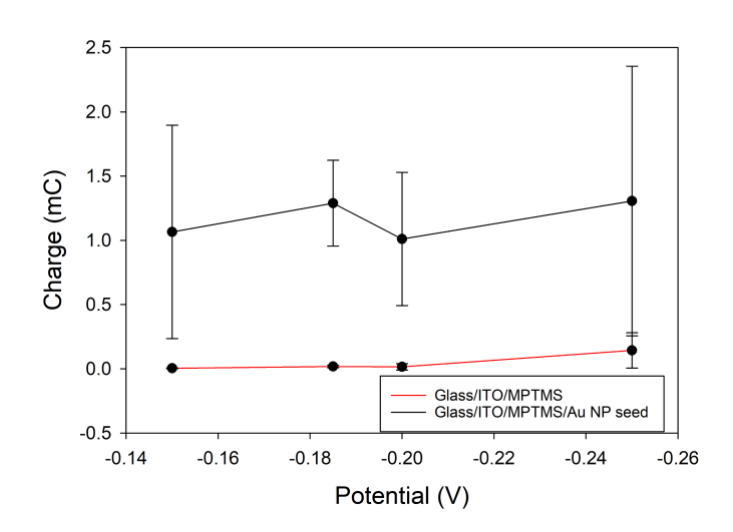


Figure 3. Charge under the ASV peak for glass/ITO/MPTMS (red) and glass/ITO/MPTMS/Au NP seed (black) electrodes held at different potentials for 60 min in pH 10.6 buffered 0.1 M CTAB plus 2.5 x 10⁻⁴ M AgNO₃ solution.

glass/ITO/MPTMS at potentials from -150 mV to about -300 mV. The amount of Ag deposited was much larger on the seeded electrode in this range because the Au NP seeds catalyze Ag deposition. At potentials more negative than -300 mV, the potential is significantly negative that nucleation and growth of Ag occurs more similarly over the entire glass/ITO/MPTMS surface and does not depend as strongly on the presence of Au NP seeds. The amount of Ag on the seeded electrodes deposited from -150 mV to -500 mV is similar based on the large error bars in the statistics. We performed two sample t-tests for seeded electrodes at potentials -185 mV vs -200 mV, -185 mV vs -300 mV and -185 mV vs -500 mV and found that there was no statistically significant difference at these three potentials at 90% confidence (p = 0.483, p = 0.78, at p =

0.57, respectively). This suggests that growth of Ag was limited by diffusion at these potentials. However, we performed two sample t-tests for both seeded and non-seeded electrodes at potentials of -150 mV, -185 mV, -200 mV, -250 mV, -300 mV, -400 mV and -500 mV. We found that for potentials from -150 mV to -300 mV they are statistically different at 90% confidence (p = 0.004, 0.003, 0.008, 0.061, 0.025, respectively).

For potentials -400 mV and -500 mV, we found that they are not statistically different at 90% confidence (p = 0.23, p = 0.309, respectively). This proves that growth of Ag occurs more similarly over the entire glass/ITO/MPTMS surface and does not depend as strongly on the presence of Au NP seeds.

Figure 3 shows the charge under the ASV peak for glass/ITO/MPTMS and glass/ITO/MPTMS/Au NP seed obtained after Ag deposition for 60 mins at -150 mV, -185 mV,

-200 mV and -250 mV. Table S2 in the Supporting Information presents the average charge statistics at these four potentials for a deposition time of 60 minutes. We focused on the potentials from -150 mV to -250 mV since these potentials appeared to have the least amount of Ag deposited on the glass/ITO/MPTMS surface. It was observed that Ag deposition was much larger at potentials from -150 mV to -250 mV

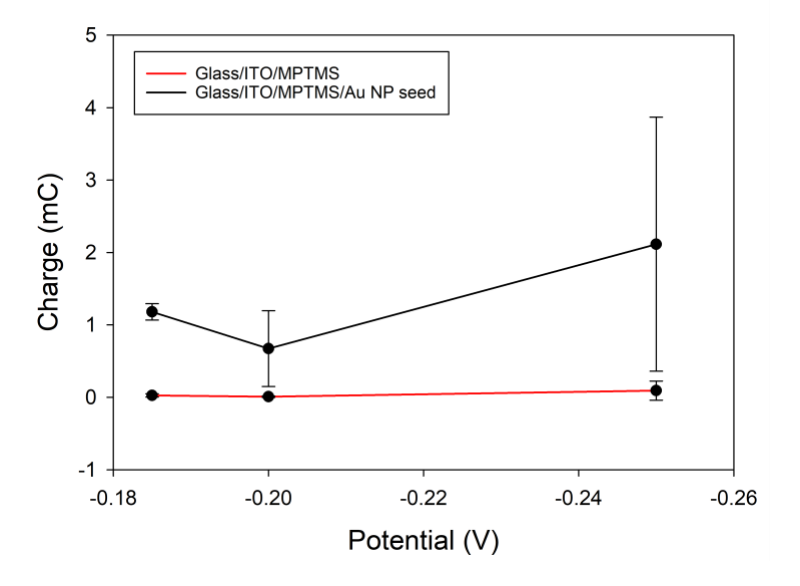


Figure 4. Anodic stripping voltammetry charge for glass/ITO/MPTMS (red) and glass/ITO/MPTMS/Au NP seed (black) electrodes after holding at different potentials for 120 min in pH 10.6 buffered 0.1 M CTAB plus 2.5 x 10⁻⁴ M AgNO₃ solution.

with almost no deposition on glass/ITO/MPTMS, indicating that seed-mediated growth occurred primarily on the seeded surfaces in this potential range. We performed two sample t-tests for both seeded and non-seeded electrodes at potentials of -150 mV, -185 mV, -200 mV and -250 mV and found that they are statistically different at 90% confidence. (p = 0.084, p = 0.022, p = 0.031, p = 0.07 respectively). This confirms that there is more Ag deposition on seeded electrodes as compared to non-seeded electrodes at these potentials.

ASV was also performed on glass/ITO/MPTMS and glass/ITO/MPTMS/Au NP after 120 minutes at potentials of -185 mV, -200 mV and -250 mV (Figure 4). Table S3 in the Supporting Information presents the average charge statistics at these three potentials for a deposition time of 120 minutes. We performed two sample t-tests for seeded electrodes at potentials -185 mV versus -200 mV and -185 mV versus -250 mV and found no statistically significant difference at 95% confidence (p = 0.118, p = 0.59 respectively). The charge was again larger for the Au NP seeded electrode and the average amount of Ag deposited increased for deposition of 120 min

(2.0 mC at -250 mV) as compared to 60 min (1.0 mC at -250 mV). Importantly there is an

insignificant amount of Ag
deposition on glass/ITO/MPTMS
for these three potentials. Twosample t-tests comparing the
means between non-seeded and
seeded electrodes at potentials 185 mV, -200 mV and -250 mV
at 90% confidence and found that
only -185 mV showed statistical
difference while it showed no
statistical difference for -200 mV
and -250 mV (p = 0.045, p =
0.159, p = 0.351, respectively).

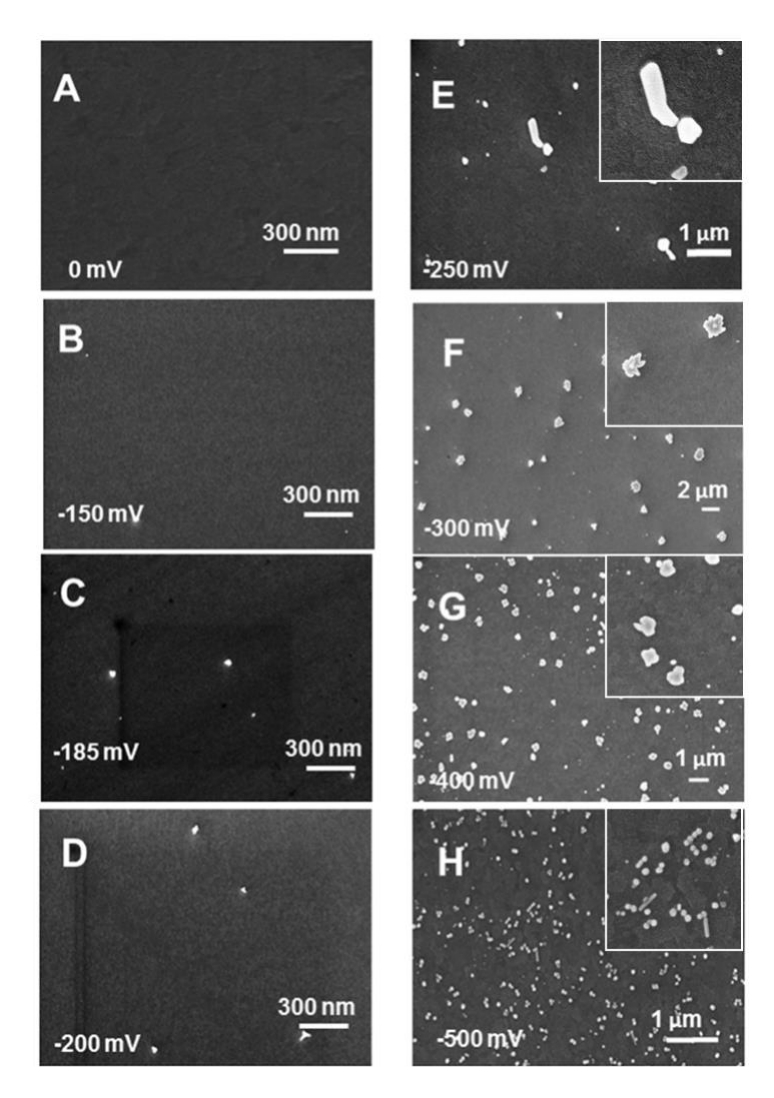


Figure 5. SEM images of glass/ITO/MPTMS at the indicated potentials after Ag deposition for 30 min at the indicated potential.

Microscopy studies. We obtained SEM images of the various glass/ITO/MPTMS and glass/ITO/MPTMS/Au NP seed electrodes at different potentials and at different time to determine the size and shape of the deposited Ag nanostructures. Figure 5 shows SEM images of the glass/ITO/MPTMS at different potentials and times. There was minimal Ag deposition on the glass/ITO/MPTMS electrodes from 0 to -250 mV, which is consistent with the ASV data. The Ag deposited in the form of branched flower like structures as seen from the insets in Figures F-H and more Ag deposited on these non-seeded electrodes at potentials from -300 mV to -500 mV, which is also consistent with the ASV charge (Figure 2B and Table S1) and SEM images in Figure S3.

Figure 6 shows glass/ITO/MPTMS and glass/ITO/MPTMS/Au seed electrodes after deposition of Ag at - 150 mV for 30, 60, and 120 min. At this potential, there were a few Ag deposits on the glass/ITO/MPTMS electrodes, consistent with the ASV data and Figure 5, and there were a significant number of Ag NRs on the glass/ITO/MPTMS/Au NP seed electrodes along with spheres and plate-shaped particles. The NR yield ranged from 5 to 10%. This

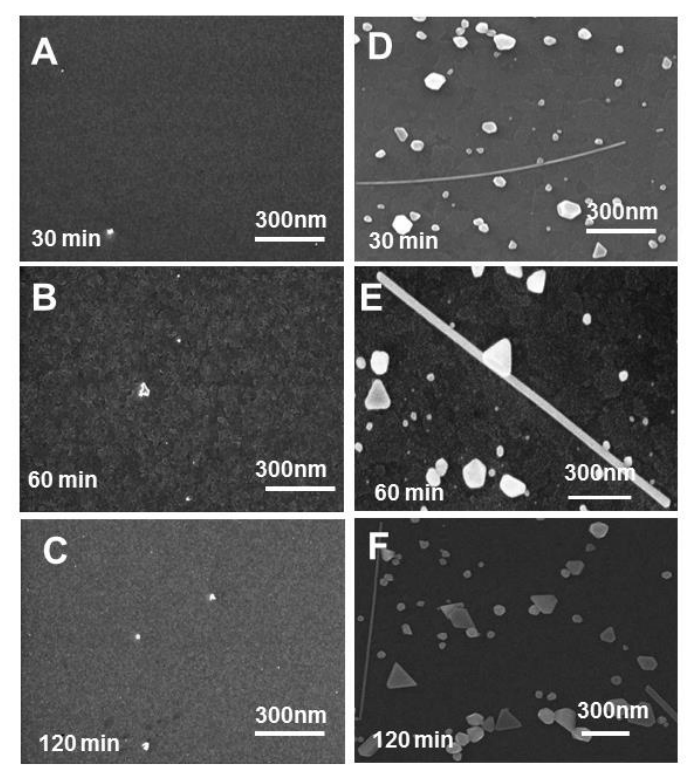


Figure 6. SEM images of glass/ITO/MPTMS (A, B, C) and glass/ITO/MPTMS/Au NP seed electrodes (D, E, F) after holding at -150 mV in Ag deposition solution for 30, 60 and 120 min.

distribution of rods, wires, spheres, and plates is similar to the seed-mediated method in CTAB

reported by Murphy and coworkers.¹⁰⁻¹³ They required centrifugation to purify the samples in solution. Our results show that Ag NRs/NWs can be formed by electrochemical seed-mediated growth in an analogous way to the formation by chemical seed-mediated growth with freely diffusing seeds in solution and ascorbic acid as a chemical reducing agent.^{32, 33}

Figure 7 shows glass/ITO/MPTMS and glass/ITO/MPTMS/Au seed electrodes after deposition of Ag at -185 mV for 30, 60, and 120 min. Again, no significant amount of Ag

deposited on the glass/ITO/MPTMS at this potential, consistent with Figures 4 and 5. Also, a significant percentage of NRs/NWs formed on the glass/ITO/MPTMS/Au NP seed electrodes. The yield of NRs/NWs ranged between 5 and 15%. There is a large size dispersity in NRs/NWs in terms of length and aspect ratio (AR). There is also a larger shape dispersity in the sample with many spherical nanoparticles and triangular or hexagonal nanoplates. NR/NW yield can be improved by using the taping method on the electrode surface

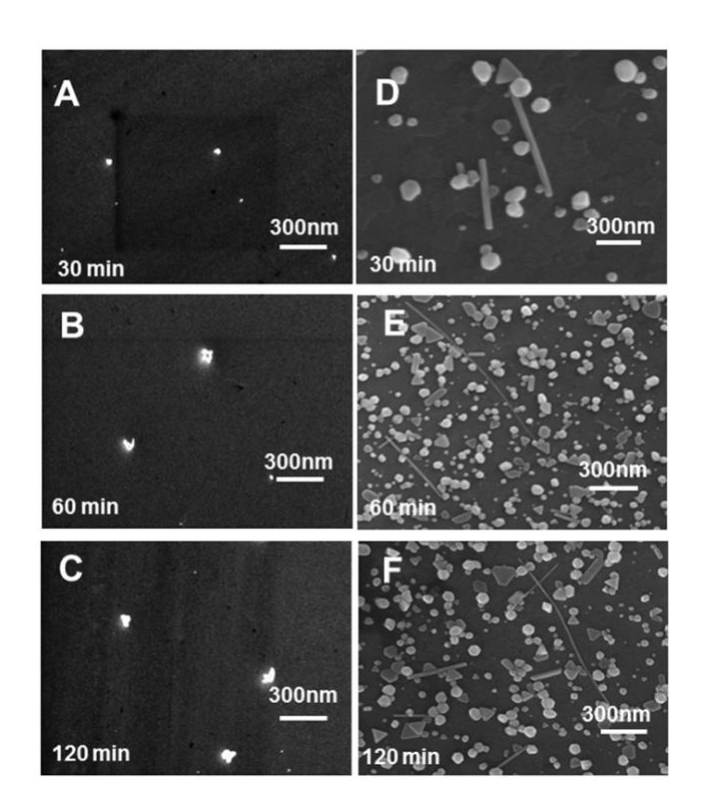


Figure 7. SEM images of glass/ITO/MPTMS (A, B, C) and glass/ITO/MPTMS/Au NP seed electrodes (D, E, F) after holding at -185 mV in Ag deposition solution for 30, 60 and 120 min.

as reported previously for chemical seed-mediated growth directly on surfaces. ^{19, 31, 34}. We performed taping on a glass/ITO/MPTMS/Au seed electrode after Ag deposition at -185 mV for 30 min by applying adhesive tape to the surface and pulling the tape back off slowly at ~90

degrees from electrode plane. Using this simple method, the Ag NR percentage increased to ~25% as shown in the Supporting Information Figure S4.

Figure 8 shows glass/ITO/MPTMS and glass/ITO/MPTMS/Au NP seed electrodes after deposition of Ag at -200 mV for 30, 60, and 120 min. Very little deposition occurred on the

electrode without Au NP seeds and Ag NRs/NWs again formed on the Au NP-seeded electrode. The yield ranged from 5-15%, similar to the deposition at -150 and -185 mV.

Table 1 compares the yield, coverage, length, and AR of the Ag NRs/NWs deposited on glass/ITO/MPTMS/Au NP seed electrodes at -150, -185 and -200 mV for 30, 60 and 120 min. The coverage of nanostructures on the surface ranged from 5 - 40 per μm² at -150 mV, 10 - 120 per

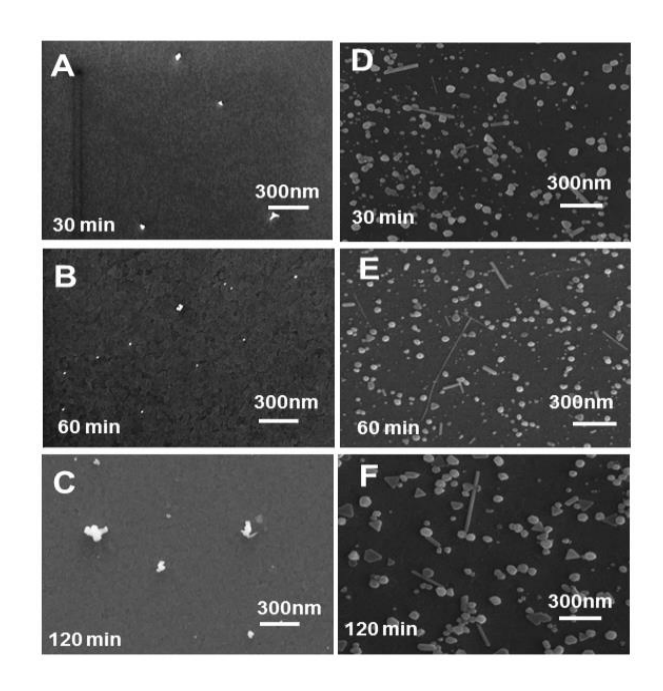


Figure 8. SEM images of glass/ITO/MPTMS (A, B, C) and glass/ITO/MPTMS/Au seed electrodes (D, E, F) after holding at -200 mV in Ag deposition solution for 30, 60 and 120 min.

 μ m² at -185 mV, and 30 - 80 per μ m² for -200 mV considering all deposition times. The density was generally higher for -185 mV and -200 mV. If only seeded growth occurs, the density should not vary. The higher density at more negative potential suggests that additional self-nucleation may have also occurred at more negative potentials. When comparing the morphology of the Ag deposited at -150, -185 and -200 mV, it is clear that the yield of NRs/NWs is higher for longer deposition times at all potentials and overall highest at -185 mV. The length and AR have very large dispersity, ranging from 200 nm to 5 μ m in length with AR ranging from

5 to 100. In general, the average length of the NRs/NWs increased from 30 to 60 min at all potentials. We found that the -150 mV and -185 mV depositions are most favorable for growing

Table 1. Statistical data on the nanorods/nanowires grown by electrochemical seed-mediated growth as a function of potential and time.

Potential (mV)	-150			-185			-200		
Time (min)	30	60	120	30	60	120	30	60	120
Yield %	2-5%	2-5%	10-12%	2-5%	5-10%	15-18%	2-5%	5-10%	12-15%
Aspect Ratio	35(±23)	57(±41)	33(±19)	11(±6)	45(±33)	35(±18)	11(±4)	41(±25)	11(±6)
Coverage	25(±12)	18(±13)	21(±7)	16(±7)	89(±41)	76(±31	68(±11)	52(±13)	51(±20)
(Particle/μm²)									
Rod Length (nm)	675(±403)	2611(±1897)	657(±366)	449(±187)	643(±472)	928(±391)	314(±100)	525(±302)	364(±150)

longer NRs/NWs and the highest AR values occurred at 60 min for all potentials. While this is a useful method for forming high AR Ag NRs and NWs electrochemically directly on electrode surfaces, the control of yield and dispersity in length and AR needs to be improved.

CONCLUSIONS

The morphology of Ag deposited on glass/ITO/MPTMS electrodes in CTAB depends on the presence or absence of Au NP seeds on the surface, the electrode potential, and the deposition time. For non-seeded glass/ITO/MPTMS electrodes, Ag deposition occurred in the form of branched or snow-flake structures at potentials ranging from -400 to -500 mV as shown in Figure S3 (Supporting Information). At 0.0 mV to -300 mV, there was very little Ag deposition on the non-seeded surface but sporadic regions with some Ag on the electrode existed. On the glass/ITO/MPTMS/Au NP seed electrodes, Ag deposition occurred from -150 mV to -500 mV and the amount of Ag deposited was greater than that on the non-seeded surfaces from -150 mV

to -250 mV. From -150 mV to -250 mV, the seed-mediated growth was optimal because there was little or no Ag deposition on non-seeded surfaces. Also, from -150 mV to -200 mV, a significant number of Ag NRs/NWs formed on the electrode surface due to the presence of CTAB. By controlling the deposition time and potential, the average NW length ranged from 300 nm to 2.6 µm and the yield ranged from 5-18%. Optimized electrochemical seed-mediated growth and the controlled formation of Ag NRs/NWs and other shaped metal nanostructures on electrode supports is important as it could lead to applications in chemical/electrochemical sensing, plasmonics, catalysis, and nanoelectronics. Controlling morphology through controlled electrode potential is a promising approach to nanostructure engineering.

Supporting Information Available

UV-Vis spectroscopy data of 4 nm Au NPs in solution, anodic stripping voltammograms (ASV), data tables with all ASV charge statistics, and SEM images after Ag deposition of seeded glass/ITO/MPTMS/Au seed, non-seeded glass/ITO/MPTMS and taped samples of glass/ITO/MPTMS/Au seed electrodes.

ACKNOWLEDGEMENTS

We gratefully acknowledge the National Science Foundation (CHE-1308763 and CHE-2004169) for financial support of this research. The facilities at the Electro-optics and Research Institute and Nanotechnology Center (ERINC) and the Conn Center for Renewable Energy Research at the University of Louisville made it possible to obtain the scanning electron microscopy (SEM) images presented in this article. We would also like to thank Indiana University Southeast for their financial support (Grant-in-Aid).

REFERENCES

- (1) Zamborini, F. P.; Bao, L.; Dasari, R. Nanoparticles in Measurement Science. *Anal. Chem.* **2012**, *84*, 541-576.
- (2) Huang, Y.; Duan, X.; Wei, Q.; Lieber, C. M. Directed Assembly of One-Dimensional Nanostructures into Functional Networks. *Science* **2001**, *291*, 630-633.
- (3) Smith, P. A.; Nordquist, C. D.; Jackson, T. N.; Mayer, T. S.; Martin, B. R.; Mbindyo, J.; Mallouk, T. E. Electric-field assisted assembly and alignment of metallic nanowires. *Appl. Phys. Lett.* **2000**, *77*, 1399-1401.
- (4) Kempa, K.; Kimball, B.; Rybczynski, J.; Huang, Z. P.; Wu, P. F.; Steeves, D.; Sennett, M.; Giersig, M.; Rao, D. V. G. L. N.; Carnahan, D. L.; et al. Photonic Crystals Based on Periodic Arrays of Aligned Carbon Nanotubes. *Nano Lett.* **2003**, *3*, 13-18.
- (5) Walter, E. C.; Zach, M. P.; Favier, F.; Murray, B. J.; Inazu, K.; Hemminger, J. C.; Penner, R. M. Metal Nanowire Arrays by Electrodeposition. *ChemPhysChem* **2003**, *4*, 131-138.
- (6) Cui, Y.; Wei, Q.; Park, H.; Lieber, C. M. Nanowire Nanosensors for Highly Sensitive and Selective Detection of Biological and Chemical Species. *Science* **2001**, *293*, 1289-1292.
- (7) Maier, S. A.; Kik, P. G.; Atwater, H. A.; Meltzer, S.; Harel, E.; Koel, B. E.; Requicha, A. A. G. Local detection of electromagnetic energy transport below the diffraction limit in metal nanoparticle plasmon waveguides. *Nat Mater* **2003**, *2*, 229-232.
- (8) Zheng, J.; Cheng, X.; Zhang, H.; Bai, X.; Ai, R.; Shao, L.; Wang, J. Gold Nanorods: The Most Versatile Plasmonic Nanoparticles. *Chem Rev* **2021**, *121*, 13342-13453.
- (9) Nikoobakht, B.; El-Sayed, M. A. Preparation and Growth Mechanism of Gold Nanorods (NRs) Using Seed-Mediated Growth Method. *Chem. Mater.* **2003**, *15*, 1957-1962.
- (10) Sau, T. K.; Murphy, C. J. Seeded High Yield Synthesis of Short Au Nanorods in Aqueous Solution. *Langmuir* **2004**, *20*, 6414-6420.
- (11) Jana, N. R.; Gearheart, L.; Murphy, C. J. Wet Chemical Synthesis of High Aspect Ratio Cylindrical Gold Nanorods. *J. Phys. Chem. B* **2001**, *105*, 4065-4067.
- (12) Jana, N. R.; Gearheart, L.; Murphy, C. J. Seed-Mediated Growth Approach for Shape-Controlled Synthesis of Spheroidal and Rod-like Gold Nanoparticles Using a Surfactant Template. *Adv. Mater.* **2001**, *13*, 1389-1393.
- (13) Johnson, C. J.; Dujardin, E.; Davis, S. A.; Murphy, C. J.; Mann, S. Growth and form of gold nanorods prepared by seed-mediated, surfactant-directed synthesis. *J. Mater. Chem.* **2002**, *12*, 1765-1770.
- (14) Mieszawska, A. J.; Jalilian, R.; Sumanasekera, G. U.; Zamborini, F. P. The Synthesis and Fabrication of One-Dimensional Nanoscale Heterojunctions. *Small* **2007**, *3*, 722-756.
- (15) Taub, N.; Krichevski, O.; Markovich, G. Growth of Gold Nanorods on Surfaces. *J. Phys. Chem. B* **2003**, *107*, 11579-11582.
- (16) Wei, Z.; Zamborini, F. P. Directly Monitoring the Growth of Gold Nanoparticle Seeds into Gold Nanorods. *Langmuir* **2004**, *20*, 11301-11304.
- (17) Wei, Z.; Mieszawska, A. J.; Zamborini, F. P. Synthesis and Manipulation of High Aspect Ratio Gold Nanorods Grown Directly on Surfaces. *Langmuir* **2004**, *20*, 4322-4326.
- (18) Mieszawska, A. J.; Slawinski, G. W.; Zamborini, F. P. Directing the Growth of Highly Aligned Gold Nanorods through a Surface Chemical Amidation Reaction. *J. Am. Chem. Soc.* **2006**, *128*, 5622-5623.

- (19) Mieszawska, A. J.; Zamborini, F. P. Gold Nanorods Grown Directly on Surfaces from Microscale Patterns of Gold Seeds. *Chem. Mater.* **2005**, *17*, 3415-3420.
- (20) Demille, T. B.; Neal, R. D.; Preston, A. S.; Liang, Z.; Oliver, A. G.; Hughes, R. A.; Neretina, S. Epitaxially aligned single-crystal gold nanoplates formed in large-area arrays at high yield. *Nano Res.* **2022**, *15*, 296-303.
- (21) Abdelmoti, L. G.; Zamborini, F. P. Potential-Controlled Electrochemical Seed-Mediated Growth of Gold Nanorods Directly on Electrode Surfaces. *Langmuir* **2010**, *26*, 13511-13521.
- (22) Kline, T. R.; Tian, M.; Wang, J.; Sen, A.; Chan, M. W. H.; Mallouk, T. E. Template-Grown Metal Nanowires. *Inorg. Chem.* **2006**, *45*, 7555-7565.
- (23) Xiang, C.; Kung, S. C.; Taggart, D. K.; Yang, F.; Thompson, M. A.; Güell, A. G.; Yang, Y.; Penner, R. M. *ACS Nano* **2008**, *2*, 1939.
- (24) Godeffroy, L.; Ciocci, P.; Lemineur, J.-F.; Kanoufi, F. Watching operando nanoscale electrochemical deposition by optical microscopy. *Curr. Opin. Electrochem.* **2022**, *36*, 101165.
- (25) Amal Raj, M.; Abraham John, S. Fast growth of gold nanorods on solid substrate using electrochemically deposited gold seeds. *Electrochem. Commun.* **2014**, *45*, 27-31.
- (26) Nambiar, H. N.; Zamborini, F. P. Size-Dependent Electrochemical Metal Growth Kinetics. *J. Phys. Chem. C* **2023**, *127*, 4087-4095.
- (27) Oh, H.; Park, Y.; Song, H. Tracking Underpotential Deposition of Copper on Individual Silver Nanocubes by Real-Time Single-Particle Plasmon Scattering Imaging. *J. Phys. Chem. C* **2020**, *124*, 20398-20409.
- (28) Elabbadi, M.; Boukouvala, C.; Hopper, E. R.; Asselin, J.; Ringe, E. Synthesis of Controllable Cu Shells on Au Nanoparticles with Electrodeposition: A Systematic in Situ Single Particle Study. *J. Phys. Chem. C* **2023**, *127*, 5044-5053.
- (29) Masitas, R. A.; Zamborini, F. P. Oxidation of Highly Unstable <4 nm Diameter Gold Nanoparticles 850 mV Negative of the Bulk Oxidation Potential. *J. Am. Chem. Soc.* **2012**, *134*, 5014-5017.
- (30) Beeram, S. R.; Zamborini, F. P. Purification of Gold Nanoplates Grown Directly on Surfaces for Enhanced Localized Surface Plasmon Resonance Biosensing. *ACS Nano* **2010**, *4*, 3633-3646.
- (31) Sławiński, G. W.; Zamborini, F. P. Synthesis and Alignment of Silver Nanorods and Nanowires and the Formation of Pt, Pd, and Core/Shell Structures by Galvanic Exchange Directly on Surfaces. *Langmuir* **2007**, *23*, 10357-10365.
- (32) Jana, N. R.; Gearheart, L.; Murphy, C. J. Wet chemical synthesis of silver nanorods and nanowires of controllable aspect ratio. *Chem. Commun.* **2001**, 617-618.
- (33) Murphy, C. J.; Gole, A. M.; Hunyadi, S. E.; Orendorff, C. J. One-Dimensional Colloidal Gold and Silver Nanostructures. *Inorg. Chem.* **2006**, *45*, 7544-7554.
- (34) Beeram, S. R.; Zamborini, F. P. Effect of Protein Binding Coverage, Location, and Distance on the Localized Surface Plasmon Resonance Response of Purified Au Nanoplates Grown Directly on Surfaces. *J. Phys. Chem. C* **2011**, *115*, 7364-7371.

TOC Graphic:

